Parametric Study of Losses in Cross-Bonded Cables: Conductors Transposed Versus Conductors Nontransposed

Prajakta Moghe and Francisco de León, *Senior Member, IEEE*

Abstract—Conductor transposition, for cross-bonded cables, is recommended in the ANSI/IEEE Standard 575-1988 as a means to reduce interference with communication systems. In this paper, it is shown that reduced interference comes at the price of increased cable losses, which is an issue not addressed in the 1998 edition of the IEEE Standard 575. Analytical formulas are obtained for the calculation of the positive-sequence resistance for transposed and not transposed conductors to shed light on the reasons why the losses increase when the conductors are transposed. It has been found that for cross-bonded cables installed in flat formations, the positive-sequence resistance of transposed conductors is always larger than that of nontransposed conductors. Parametric studies are performed by varying all of the construction and installation parameters that affect the value of the positive-sequence resistance. In particular, we have changed the separation distance between cables, the insulation thickness, the number and resistance of the concentric wires, and the resistivity of the soil among other parameters. Examples on transmission and distribution cables are discussed.

Index Terms—Ampacity, cable parameters, cross-bonding, losses, positive-sequence impedance, resistance.

Nomenclature

r_a	Resistance of conductor of phase a (Ω/km).
r_b	Resistance of conductor of phase b (Ω/km).
r_c	Resistance of conductor of phase c (Ω/km).
r	Average value of the three-phase conductor resistances (Ω/km).
G_w	Geometric mean radius of the concentric wires (in meters).
r_w	Average value of the resistance of the concentric wires (Ω/km).
d	Distance between two consecutive conductors (in meters).
s	Number of strands of the concentric wires.
S_1	$\ln\left(850.59964 \times e^{4.26198/s} \times (0.056085^s s)^{-1/s}\right)$.
S_2	$\ln(2.35294 \times 0.01409^{1/s}(0.056085^s s)^{1/s})$.
S_3	$\ln(e^{4.26198/s}(e^{-2.88089s}s)^{-1/s})$.
IT	Insulation thickness ($\times 10^{-3}$m).
ρ	Electrical resistivity of earth ($\Omega - $m).
f	Frequency = 60 Hz
k_1	$\pi^2 \times 10^{-4} = 9.8696044 \times 10^{-4}$.
k_2	$4\pi \times 10^{-4} = 1.256637 \times 10^{-4}$.
k_3	658.87165.
k_4	$(1/2)\mathrm{e}^{-0.25} = 0.38940039156$.
Di_i	Internal diameter of the (concentric wires) layer (in meters).
De_i	External diameter of the (concentric wires) layer (in meters).
Th_i	Thickness of the layer = Diameter of concentric wires (in meters).
k	$k_3\sqrt{\rho/f} = 7.7459$.
α_i	Factor to obtain the GMR (see Table II.
GMR	Geometrical mean radius.

I. Introduction

IN A previous study [1], it has been shown that transposing the conductors of cross-bonded cables can increase the positive-sequence resistance by 20%. The study was purely numerical and offered no insight on the reasons for this counterintuitive phenomenon to happen. This fact, however, is very important because the losses of a power cable, operating under balanced conditions, are caused according to Joule's Law, by the positive-sequence resistance and the positive-sequence current computed as $3R_1 I_1^2$.

Conductor transposition, for cross-bonded cables, is advocated in the ANSI/IEEE Standard 575-1988 [2] to prevent interference with communication cables (see Appendix D3 of the standard). However, no attention is paid to the fact that the losses substantially increase by transposing the cables.

This paper presents a parametric study of the effects of conductor transposition on the losses of a three-phase cable system distributed in a flat formation.

The parametric study is carried out with the analytically derived equations for the positive-sequence resistance of cables with conductors transposed and with conductors nontransposed.
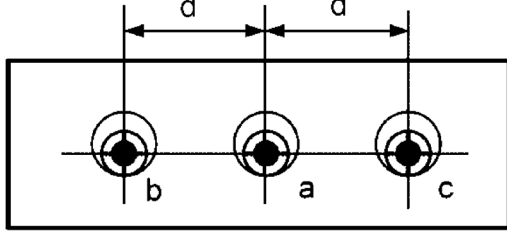
Fig. 1. Cable installation in flat formation.

A comparison is made between the values of the positive-sequence resistance from these two equations. This is done by varying only one parameter at a time for the given equation and substituting constant values for the remaining parameters. The variation of the positive-sequence resistance for both conductors transposed and nontransposed for that one particular parameter is then plotted over a wide range of values.

The parameters that are varied one at a time include the separation distance between the cables, the insulation thickness, the number of strands of the concentric wires, the resistance of the conductors, and the resistivity of the soil. Then, the values of the positive-sequence resistances are compared for each of these parameters. It is found that the value of the positive-sequence resistance remains larger for cables with transposed conductors compared to the nontransposed conductors in all cases.

II. ANALYTICAL CALCULATION OF CABLE PARAMETERS

The calculation of the cable parameters is performed by following the method described in [3] (slightly improved to account for skin and proximity effects, which are not considered in [3]).

A. Primitive Impedance Matrix

The elements of the primitive matrix are computed using Carson's equations as in [3], but the conductor resistances are computed per IEC 60287-1-1 [4]. The geometrical mean radius (GMR) is computed using the IEC Standard 60287-1-3 [5]. See [1] for a numerical example. All of these techniques are combined to produce the most accurate yet available calculation of the impedance parameters of the cable (at a power frequency of 60/50 Hz).

The input data are the geometrical information of the cable installation including the construction details of all cables in the installation. Every metallic layer of each cable (conductor, sheath, concentric wires, and armor) is explicitly represented. Thus, for a three-phase concentric cable installation as shown in Fig. 1, the primitive 6×6 impedance matrix is composed of the following 3×3 submatrices:

$$Z_{\text{primitive}} = \begin{bmatrix} [Z_{\text{primitive}}^{\text{cc}}] & [Z_{\text{primitive}}^{\text{cw}}] \\ [Z_{\text{primitive}}^{\text{wc}}] & [Z_{\text{primitive}}^{\text{ww}}] \end{bmatrix}. \quad (1)$$

where the super indices c and w represent conductors and concentric wires, respectively. The self impedances of the phase conductors (the diagonal elements of the $[Z_{\text{primitive}}]$ submatrix) are computed from

$$Z_{ii}^{\text{cc}} = (r_i + k_1 f) + jk_2 f \ln\left(\frac{k_3}{\alpha_i R_i}\sqrt{\frac{\rho}{f}}\right). \quad (2)$$

Concentric wires are treated as in Kersting [3]. Then, the diagonal elements of the submatrix $[Z_{\text{primitive}}^{\text{ww}}]$ can be computed with the modified equations from Carson by substituting the product $\alpha_i R_i$ by the geometrical mean radius as follows:

$$Z_{ii}^{\text{ww}} = (r_{wi} + k_1 f) + jk_2 f \ln\left(\frac{k_3}{\text{GMR}w_i}\sqrt{\frac{\rho}{f}}\right) \quad (3)$$

where

$$\text{GMR}w_i = \sqrt[n]{k_4 Th_i n R_i^{n-1}}$$
$$R_i = \frac{1}{2}(De_i + Di_i) \text{ and } Th_i = \frac{1}{2}(De_i - Di_i). \quad (4)$$

The offdiagonal elements of all submatrices can be computed from

$$Z_{ij} = k_1 f + jk_2 f \ln\left(\frac{k_3}{d_{ij}}\sqrt{\frac{\rho}{f}}\right). \quad (5)$$

Then, a 6×6 primitive impedance matrix can be constructed as

$$Z_{\text{primitive}} = \begin{bmatrix} Z_{\text{aa}}^{\text{cc}} & Z_{\text{ab}}^{\text{cc}} & Z_{\text{ac}}^{\text{cc}} & Z_{\text{aa}}^{\text{cw}} & Z_{\text{ab}}^{\text{cw}} & Z_{\text{ac}}^{\text{cw}} \\ Z_{\text{ab}}^{\text{cc}} & Z_{\text{bb}}^{\text{cc}} & Z_{\text{bc}}^{\text{cc}} & Z_{\text{ab}}^{\text{cw}} & Z_{\text{bb}}^{\text{cw}} & Z_{\text{bc}}^{\text{cw}} \\ Z_{\text{ac}}^{\text{cc}} & Z_{\text{bc}}^{\text{cc}} & Z_{\text{cc}}^{\text{cc}} & Z_{\text{ac}}^{\text{cw}} & Z_{\text{bc}}^{\text{cw}} & Z_{\text{cc}}^{\text{cw}} \\ Z_{\text{aa}}^{\text{wc}} & Z_{\text{ab}}^{\text{wc}} & Z_{\text{ac}}^{\text{wc}} & Z_{\text{aa}}^{\text{ww}} & Z_{\text{ab}}^{\text{ww}} & Z_{\text{ac}}^{\text{ww}} \\ Z_{\text{ab}}^{\text{wc}} & Z_{\text{bb}}^{\text{wc}} & Z_{\text{bc}}^{\text{wc}} & Z_{\text{ab}}^{\text{ww}} & Z_{\text{bb}}^{\text{ww}} & Z_{\text{bc}}^{\text{ww}} \\ Z_{\text{ac}}^{\text{wc}} & Z_{\text{bc}}^{\text{wc}} & Z_{\text{cc}}^{\text{wc}} & Z_{\text{ac}}^{\text{ww}} & Z_{\text{bc}}^{\text{ww}} & Z_{\text{cc}}^{\text{ww}} \end{bmatrix}. \quad (6)$$

Note that $Z_{\text{primitive}}$ and all if its submatrices are symmetric.

B. Cross-Bonding—Reduction to Phase Conductors

The primitive impedance matrix is reduced to phase conductors taking into consideration the bonding type. For the case of cross-bonded concentric wires with equal minor section lengths and phase conductors not transposed (NT), the first step is to permute the matrix and take the corresponding averages yielding

$$Z_{\text{bond}}^{\text{NT}} = \begin{bmatrix} Z_{\text{aa}}^{\text{cc}} & Z_{\text{ab}}^{\text{cc}} & Z_{\text{ac}}^{\text{cc}} & Z_{\text{a}}^{\text{cw}} & Z_{\text{a}}^{\text{cw}} & Z_{\text{a}}^{\text{cw}} \\ Z_{\text{ab}}^{\text{cc}} & Z_{\text{bb}}^{\text{cc}} & Z_{\text{bc}}^{\text{cc}} & Z_{\text{b}}^{\text{cw}} & Z_{\text{b}}^{\text{cw}} & Z_{\text{b}}^{\text{cw}} \\ Z_{\text{ac}}^{\text{cc}} & Z_{\text{bc}}^{\text{cc}} & Z_{\text{cc}}^{\text{cc}} & Z_{\text{c}}^{\text{cw}} & Z_{\text{c}}^{\text{cw}} & Z_{\text{c}}^{\text{cw}} \\ Z_{\text{a}}^{\text{wc}} & Z_{\text{b}}^{\text{wc}} & Z_{\text{c}}^{\text{wc}} & Z_{\text{s}}^{\text{ww}} & Z_{\text{m}}^{\text{ww}} & Z_{\text{m}}^{\text{ww}} \\ Z_{\text{a}}^{\text{wc}} & Z_{\text{b}}^{\text{wc}} & Z_{\text{c}}^{\text{wc}} & Z_{\text{m}}^{\text{ww}} & Z_{\text{s}}^{\text{ww}} & Z_{\text{m}}^{\text{ww}} \\ Z_{\text{a}}^{\text{wc}} & Z_{\text{b}}^{\text{wc}} & Z_{\text{c}}^{\text{wc}} & Z_{\text{m}}^{\text{ww}} & Z_{\text{m}}^{\text{ww}} & Z_{\text{s}}^{\text{ww}} \end{bmatrix}$$

$$= \begin{bmatrix} [Z_{\text{bondNT}}^{\text{cc}}] & [Z_{\text{bondNT}}^{\text{cw}}] \\ [Z_{\text{bondNT}}^{\text{wc}}] & [Z_{\text{bondNT}}^{\text{ww}}] \end{bmatrix} \quad (7)$$

where the elements of matrix (7) are computed from the elements of matrix (6) as

$$Z_{\mathrm{a}}^{\mathrm{cw}} = \frac{(Z_{\mathrm{aa}}^{\mathrm{cw}} + Z_{\mathrm{ab}}^{\mathrm{cw}} + Z_{\mathrm{ac}}^{\mathrm{cw}})}{3}$$

$$Z_{\mathrm{b}}^{\mathrm{cw}} = \frac{(Z_{\mathrm{ab}}^{\mathrm{cw}} + Z_{\mathrm{bb}}^{\mathrm{cw}} + Z_{\mathrm{bc}}^{\mathrm{cw}})}{3}$$

$$Z_{\mathrm{c}}^{\mathrm{cw}} = \frac{(Z_{\mathrm{ac}}^{\mathrm{cw}} + Z_{\mathrm{bc}}^{\mathrm{cw}} + Z_{\mathrm{cc}}^{\mathrm{cw}})}{3}$$

$$Z_{\mathrm{s}}^{\mathrm{ww}} = \frac{(Z_{\mathrm{aa}}^{\mathrm{ww}} + Z_{\mathrm{bb}}^{\mathrm{ww}} + Z_{\mathrm{cc}}^{\mathrm{ww}})}{3}$$

$$Z_{\mathrm{m}}^{\mathrm{ww}} = \frac{(Z_{\mathrm{ab}}^{\mathrm{ww}} + Z_{\mathrm{ac}}^{\mathrm{ww}} + Z_{\mathrm{bc}}^{\mathrm{ww}})}{3}.$$

Note that in (7), the $[Z_{\mathrm{bondNT}}^{\mathrm{cc}}]$ submatrix is not different from $[Z_{\mathrm{primitive}}^{\mathrm{cc}}]$; submatrix $[Z_{\mathrm{bondNT}}^{\mathrm{ww}}]$ has only two different numbers, one for the self (s) and one for the mutual (m) elements. The submatrices $[Z_{\mathrm{bondNT}}^{\mathrm{cw}}]$ and $[Z_{\mathrm{bondNT}}^{\mathrm{wc}}]$ are symmetric and have only three different values, one per row or column, respectively.

For the case where the conductors are (counter-) transposed (T), the impedance matrix after applying bonding (permutation and averaging) becomes

$$Z_{\mathrm{bond}}^{\mathrm{T}} = \begin{bmatrix} Z_{\mathrm{s}}^{\mathrm{cc}} & Z_{\mathrm{m}}^{\mathrm{cc}} & Z_{\mathrm{m}}^{\mathrm{cc}} & Z_{\mathrm{aaT}}^{\mathrm{cw}} & Z_{\mathrm{abT}}^{\mathrm{cw}} & Z_{\mathrm{acT}}^{\mathrm{cw}} \\ Z_{\mathrm{m}}^{\mathrm{cc}} & Z_{\mathrm{s}}^{\mathrm{cc}} & Z_{\mathrm{m}}^{\mathrm{cc}} & Z_{\mathrm{abT}}^{\mathrm{cw}} & Z_{\mathrm{bbT}}^{\mathrm{cw}} & Z_{\mathrm{bcT}}^{\mathrm{cw}} \\ Z_{\mathrm{m}}^{\mathrm{cc}} & Z_{\mathrm{m}}^{\mathrm{cc}} & Z_{\mathrm{s}}^{\mathrm{cc}} & Z_{\mathrm{acT}}^{\mathrm{cw}} & Z_{\mathrm{bcT}}^{\mathrm{cw}} & Z_{\mathrm{ccT}}^{\mathrm{cw}} \\ Z_{\mathrm{aaT}}^{\mathrm{wc}} & Z_{\mathrm{abT}}^{\mathrm{wc}} & Z_{\mathrm{acT}}^{\mathrm{wc}} & Z_{\mathrm{s}}^{\mathrm{ww}} & Z_{\mathrm{m}}^{\mathrm{ww}} & Z_{\mathrm{m}}^{\mathrm{ww}} \\ Z_{\mathrm{abT}}^{\mathrm{wc}} & Z_{\mathrm{bbT}}^{\mathrm{wc}} & Z_{\mathrm{bcT}}^{\mathrm{wc}} & Z_{\mathrm{m}}^{\mathrm{ww}} & Z_{\mathrm{s}}^{\mathrm{ww}} & Z_{\mathrm{m}}^{\mathrm{ww}} \\ Z_{\mathrm{acT}}^{\mathrm{wc}} & Z_{\mathrm{bcT}}^{\mathrm{wc}} & Z_{\mathrm{ccT}}^{\mathrm{wc}} & Z_{\mathrm{m}}^{\mathrm{ww}} & Z_{\mathrm{m}}^{\mathrm{ww}} & Z_{\mathrm{s}}^{\mathrm{ww}} \end{bmatrix}$$

$$= \begin{bmatrix} [Z_{\mathrm{bondT}}^{\mathrm{cc}}] & [Z_{\mathrm{bondT}}^{\mathrm{cw}}] \\ [Z_{\mathrm{bondT}}^{\mathrm{wc}}] & [Z_{\mathrm{bondT}}^{\mathrm{ww}}] \end{bmatrix} \quad (8)$$

where the elements of (8) are computed from the elements of (6) as

$$Z_{\mathrm{s}}^{\mathrm{cc}} = \frac{(Z_{\mathrm{aa}}^{\mathrm{cc}} + Z_{\mathrm{bb}}^{\mathrm{cc}} + Z_{\mathrm{cc}}^{\mathrm{cc}})}{3}$$

$$Z_{\mathrm{m}}^{\mathrm{cc}} = \frac{(Z_{\mathrm{ab}}^{\mathrm{cc}} + Z_{\mathrm{ac}}^{\mathrm{cc}} + Z_{\mathrm{bc}}^{\mathrm{cc}})}{3}$$

$$Z_{\mathrm{aaT}}^{\mathrm{cw}} = \frac{(Z_{\mathrm{aa}}^{\mathrm{cw}} + Z_{\mathrm{bc}}^{\mathrm{cw}} + Z_{\mathrm{bc}}^{\mathrm{cw}})}{3}$$

$$Z_{\mathrm{abT}}^{\mathrm{cw}} = \frac{(Z_{\mathrm{ab}}^{\mathrm{cw}} + Z_{\mathrm{cc}}^{\mathrm{cw}} + Z_{\mathrm{ab}}^{\mathrm{cw}})}{3}$$

$$Z_{\mathrm{acT}}^{\mathrm{cw}} = \frac{(Z_{\mathrm{ac}}^{\mathrm{cw}} + Z_{\mathrm{ac}}^{\mathrm{cw}} + Z_{\mathrm{bb}}^{\mathrm{cw}})}{3}$$

$$Z_{\mathrm{bbT}}^{\mathrm{cw}} = \frac{(Z_{\mathrm{bb}}^{\mathrm{cw}} + Z_{\mathrm{ac}}^{\mathrm{cw}} + Z_{\mathrm{ac}}^{\mathrm{cw}})}{3}$$

$$Z_{\mathrm{bcT}}^{\mathrm{cw}} = \frac{(Z_{\mathrm{bc}}^{\mathrm{cw}} + Z_{\mathrm{aa}}^{\mathrm{cw}} + Z_{\mathrm{bc}}^{\mathrm{cw}})}{3}$$

$$Z_{\mathrm{ccT}}^{\mathrm{cw}} = \frac{(Z_{\mathrm{cc}}^{\mathrm{cw}} + Z_{\mathrm{ab}}^{\mathrm{cw}} + Z_{\mathrm{ab}}^{\mathrm{cw}})}{3}.$$

One can note that now in addition to having $[Z_{\mathrm{bondT}}^{\mathrm{ww}}]$ with only self and one for the mutual elements, submatrix $[Z_{\mathrm{bondT}}^{\mathrm{cc}}]$ is reduced to self and mutual elements as well. Also note that as visible in (8), submatrices $[Z_{\mathrm{bondT}}^{\mathrm{cw}}]$ and $[Z_{\mathrm{bondT}}^{\mathrm{wc}}]$ are symmetric. However, they have now six numerically different elements rather than only three as in the nontransposed case (7).

The submatrices corresponding to the concentric wires can be eliminated using the Kron reduction (since the wires are grounded on both sides). This reduction is done with

$$Z_{abc} = [Z^{cc}] - [Z^{cw}][Z^{ww}]^{-1}[Z^{wc}] \quad (9)$$

yielding a 3×3 phase matrix for the nontransposed and transposed cases.

C. Symmetrical Components Transformation

The final step in computing the positive-sequence resistance is to apply the symmetrical components transformation as follows:

$$Z_{012} = T^{-1} Z_{abc} T \quad (10)$$

where

$$T = \begin{bmatrix} 1 & 1 & 1 \\ 1 & a^2 & a \\ 1 & a & a^2 \end{bmatrix}.$$

In agreement with [3] for the transposed case, we find perfect decoupling between the sequences. Therefore, the sequence impedance matrix becomes

$$ZT_{012} = \begin{bmatrix} Z_{T0} & & \\ & Z_{T1} & \\ & & Z_{T2} \end{bmatrix}. \quad (11)$$

For the nontransposed case, the decoupling is not perfect and mutual couplings between sequences exist as follows:

$$ZNT_{012} = \begin{bmatrix} Z_{NT0} & Z_{NT01} & Z_{T02} \\ Z_{NT10} & Z_{NT1} & Z_{T12} \\ Z_{NT20} & Z_{T21} & Z_{NT2} \end{bmatrix}. \quad (12)$$

In general, the offdiagonal elements of the nontransposed sequence impedance matrix are (much) smaller than the diagonal elements, but they are not zero.

The positive-sequence resistance is then obtained from the positive-sequence impedance (Z_{T1} and Z_{NT1}) by separating the real part as

$$R_{1(T)} = \mathrm{Re}[Z_{T1}]; \quad R_{1(NT)} = \mathrm{Re}[Z_{NT1}]. \quad (13)$$

The positive-sequence resistance for conductors nontransposed can be obtained analytically by performing the matrix operations in (12) and (13) yielding (14) at the bottom of the next page.

The values of constants A_1 to A_3 can be found in the Appendix. From (14), shown at the bottom of the next page, we can see that the positive-sequence resistance for conductors nontransposed is comprised of two terms. The first term represents the average value of the three-phase conductor resistances $r = (r_a + r_b + r_c)/3$. The second term is a fraction that depends on the average value of the resistances of the concentric wires, the distance between the two consecutive copper conductors, and the GMR of the concentric wires.

The positive-sequence resistance for the case of transposed conductors has an analytical formula extending several pages and it cannot be presented in this paper. In the following section, we present a parametric analysis comparing the parameters that

Conductor diameter = 56 mm
Conductor shield diameter = 62.4 mm
Insulation diameter = 106.4 mm
Insulation screen diameter = 110.14 mm
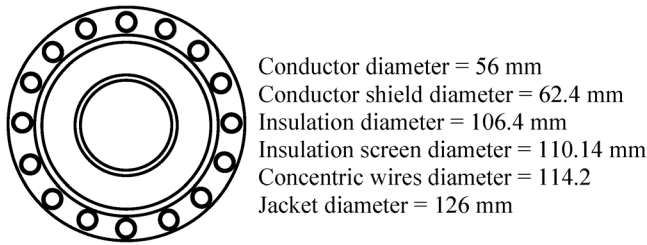Concentric wires diameter = 114.2
Jacket diameter = 126 mm

Fig. 2. Cable construction details.

affect the value of the positive-sequence resistance for cases when one geometrical value is varied at a time.

One can note that always

$$R_{1(T)} > R_{1(NT)}. \tag{15}$$

Therefore, the losses of the transposed cables are always larger than the losses of the nontransposed cables.

III. PARAMETRIC STUDY

A parametric study is presented on the variation of the positive-sequence resistance of cables with conductors transposed and nontransposed, varying one parameter at a time.

A typical 220-kV installation used in Red Eléctrica de España (Spanish TSO) is considered for the analysis as in [1]. The three cables are installed in a flat formation and are separated by a distance of $d = 0.425$ m. The cable construction details is as shown in Fig. 2.

A. Changing the Separation Distance Between Cables

Consider the parametric equation of the positive-sequence resistance for conductors transposed and conductors nontransposed. By substituting the numerical values of all the parameters for the given cable except for the distance d between the consecutive conductors, we derive the equation of the positive-sequence resistance in terms of the distance between the conductors. The positive-sequence resistance for conductors transposed becomes (16), shown at the bottom of the page.

The values of constants A_4 to A_{20} can be found in the Appendix. The positive-sequence resistance for conductors not transposed is

$$R_{1(NT\_d)} = A_{21} + [A_{22}/\{A_{23} + [A_{24} + A_{25}L_1]L_1\}] \tag{17}$$

where $L_1 = \ln(1/d)$.

The distance between the two consecutive conductors is varied from 10^{-4} (almost touching) to 1 m. The positive-sequence resistance is plotted for conductors transposed and conductors not transposed in Fig. 3. One can see that the positive-sequence resistance for conductors not transposed does not change; it remains constant at the average value r. However, the positive-sequence resistance for the transposed case changes substantially as the distance varies. The minimum value attained is r, for $d = 0$ and $d = \infty$. Therefore, for all practical separation distances between cables, transposing cables increases the losses.

B. Changing the Insulation Thickness

The geometric mean radius of the phase conductor and a neutral strand G_w depends on three factors, one of which is the insulation thickness. Thus, changing the thickness of the insulation changes G_w which, in turn, varies the positive-sequence resistance of the cable. The equations for the positive-sequence resistance in terms of the insulation thickness for conductors transposed are shown in (18) at the bottom of the next page and for conductors not transposed is

$$R_{1(NT\_IT)} =$$
$$A_{21} + \left[A_{22}/\{A_{44} - A_{45}[-A_{46} - 3C_3][A_{47} + C_3]\}\right] \tag{19}$$

where

$$C_1 = \ln\left((34.285 + IT)^{(s-1)}\right)$$
$$C_2 = \ln\left(\frac{1}{(34.285 + IT)^{\left(\frac{s-1}{s}\right)}}\right)$$
$$C_3 = \ln\left(\frac{806820.016197}{(34.285 + IT)^{\left(\frac{s-1}{s}\right)}}\right)$$

$$R_{1(NT)} = r + \frac{A_1 A_2 A_3^2}{9A_1^2 + 4A_2 A_3^2 - 3A_2\left[4A_3 - 6\ln\left(\frac{k}{d}\right) - 3\ln\left(\frac{k}{G_w}\right)\right]\left[2\ln\left(\frac{k}{d}\right) + \ln\left(\frac{k}{G_w}\right)\right]}. \tag{14}$$

$$R_{1(T\_d)} = \frac{\{A_4 + L_1[A_5 + L_1[A_6 + L_1[A_7 + L_1[A_8 + L_1[A_9 + A_{10}L_1]]]]]\}}{\left\{\begin{array}{l}[A_{11} + L_1[A_{12} + A_{13}L_1]][A_{14} + L_1[A_{15} + A_{16}L_1]] \\ [A_{17} + A_{18}\ln\left(\frac{1}{d^2}\right) + L_1[A_{19} + A_{20}L_1]]\end{array}\right\}}. \tag{16}$$
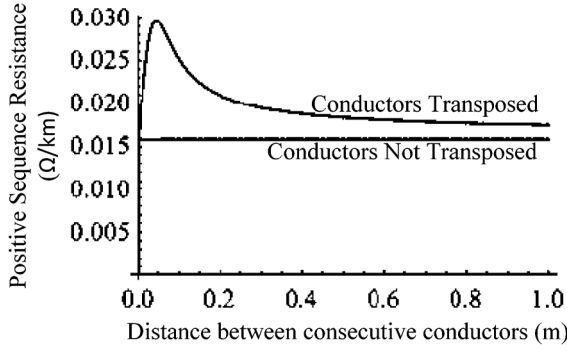
Fig. 3. Variation of the positive-sequence resistance for conductors transposed and conductors not transposed with respect to distance between consecutive conductors.
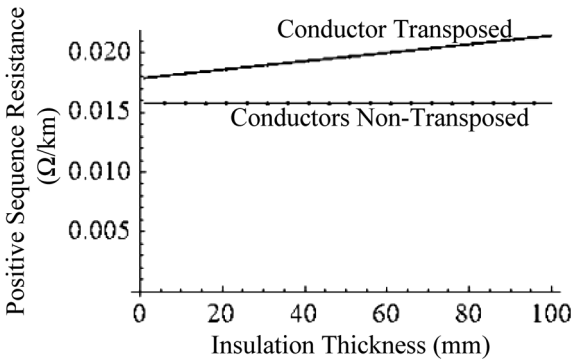

Fig. 4. Variation of positive-sequence resistance for conductors transposed and conductors not transposed with respect to the insulation thickness.

for $s = 78 =$ number of strands of concentric wires. The values of the constants A are given in the Appendix.

The variation in the positive-sequence resistance for the two cross bonding alternatives of cables is plotted in Fig. 4 when varying the insulation thickness from 1 to 100 mm. As in the previous case, one can see that for conductors not transposed, the positive resistance remains constant at the average value r, while the positive-sequence resistance for the transposed case changes substantially as the insulation thickness varies and it is always larger than r. Therefore, transposing cables increases the losses regardless of the cable insulation thickness.

On increasing the insulation thickness above 100 mm, the variation in the positive-sequence resistance for conductors transposed is similar to the variation of the positive-sequence resistance for conductors transposed when the separation distance between the cables is changed as seen in Fig. 4. Results are not shown since thicker insulation is not practical.

C. Varying the Number of Strands in the Concentric Wires

In addition to the insulation thickness, the geometric mean radius of the phase conductor and a neutral strand G_w also depends on the number of strands in the concentric wires. The equations for the positive-sequence resistance in terms of the number of strands of the concentric wires for conductors transposed are shown in (20), at the bottom of the page, and conductors not transposed are shown as

$$R_{1(NT\_s)} = A_{21} + \left[A_{22}/\left\{A_{66} + A_{67}S_3 + A_{68}S_3^2\right\}\right] \quad (21)$$

where $S_4 = \ln(0.00276621 e^{-8.52397/s}(0.056085^s s)^{2/s})$.

The positive-sequence resistance for the two cables is plotted in Fig. 5 when the number of strands is varied from 5 to 200. It can be seen, once again, that the positive-sequence resistance of cables with nontransposed conductors remains unchanged at the average resistance r. As the number of strands in the concentric wires increases, the positive-sequence resistance of transposed cables increases. For cables with more than a few concentric wires, the positive-sequence resistance remains virtually unchanged as the number of wires increases, but at a higher value than for the case when the conductors are not transposed.

D. Equating the Resistance of Conductors

From the previous results, we suspected that the differences could come from the fact that the resistances of the conductors of different phases are slightly different. This is so because the attained temperature is different (the center cable is always slightly hotter). In this subsection we assume that the resistance of all the three conductors is the same $r = r_a = r_b = r_c$. Under those conditions, we are able to express the positive-sequence resistances in terms of the resistances of the conductors as follows:

$$R_{1(T\_r)} = A_{69} + A_{70}r \quad (22)$$

$$R_{1(NT\_r)} = A_{71} + r \quad (23)$$

$$R_{1(T\_IT)} = \frac{\left\{A_{26} - A_{27}C_3 + A_{28}C_3^2 + A_{29}C_3^3 - A_{30}C_3^4 + A_{31}C_3^6 + A_{32}C_1\right\}}{\left\{\begin{array}{l}\left[A_{33} - A_{34}C_3 + A_{35}C_3^2 - A_{36}C_1\right]\left[A_{37} - A_{38}C_3 + A_{39}C_3^2 - A_{40}C_1\right]\\ \left[A_{41} + A_{42}C_2 + A_{43}C_2^2\right]\end{array}\right\}} \quad (18)$$

$$R_{1(T\_s)} = \frac{\left\{A_{48} + A_{49}S_4 - A_{50}S_1 + A_{51}S_1^2 + A_{52}S_1^3 - A_{53}S_1^4 + A_{54}S_1^6\right\}}{\left\{\begin{array}{l}\left[A_{55} + A_{56}S_3 + A_{57}S_3^2\right]\left[A_{58} - A_{59}S_1 + A_{60}S_1^2 - A_{61}S_2\right]\\ \left[A_{62} - A_{63}S_1 + A_{64}S_1^2 - A_{65}S_2\right]\end{array}\right\}} \quad (20)$$
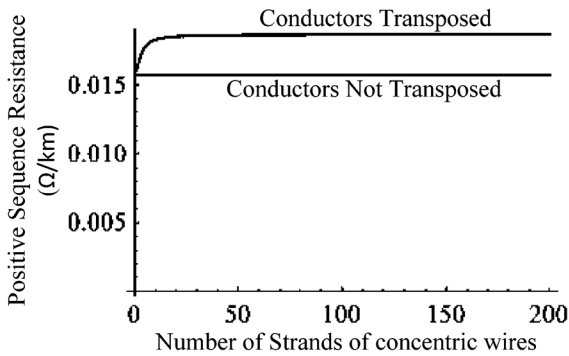
Fig. 5. Variation of positive-sequence resistance for conductors transposed and conductors not transposed with respect to the number of strands in the concentric wires.
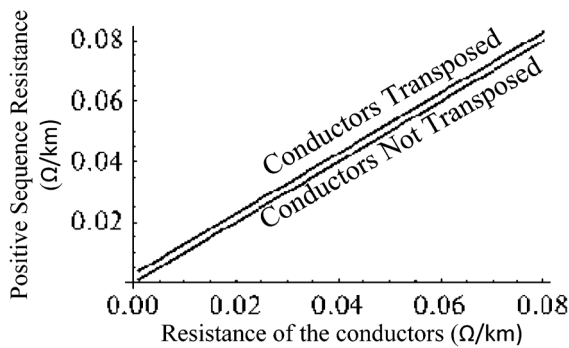

Fig. 6. Variation of positive-sequence resistance for conductors transposed and conductors not transposed with respect to the resistance of the copper conductors.

where r = resistance of the copper conductors at a fixed temperature; $A_{69} = 2.89512 \times 10^{-3}$; $A_{70} = 999999$; $A_{71} = 2.33112 \times 10^{-5}$.

From (23), it can be easily seen that the positive-sequence resistance for the conductors not transposed is larger than the conductor resistance by $2.33112 \times 10^{-5} \Omega/\mathrm{km}$. From (22), it can be seen that the positive-sequence resistance of the cables with conductors transposed is larger than the conductor resistance by approximately $2.89512 \times 10^{-3} \Omega/\mathrm{km}$. Therefore, it is possible to conclude that positive-sequence resistance of the cables with transposed conductors is always greater than the positive-sequence resistance of the cables with conductors not transposed.

The variation in the positive-sequence resistance for the conductors transposed and conductors not transposed with respect to the change in the conductor resistance is plotted in Fig. 6. As expected from (22) and (23), the difference is only a constant, but the positive-sequence resistance for cables with transposed
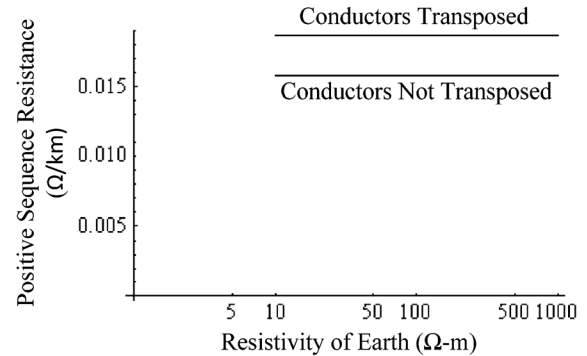

Fig. 7. Variation of positive-sequence resistance for conductors transposed and conductors not transposed with respect to the resistivity of the soil.

conductors is always larger than that of cables with nontransposed conductors.

E. Changing the Resistivity of the Soil

From (3), we can see that the constant k in the positive-sequence resistance equation for conductors not transposed is composed of three factors which are the constant k_3, the frequency, and the resistivity of the soil. Thus, varying the resistivity of the soil will affect the positive-sequence resistance.

The equation of the positive-sequence resistance for conductors transposed and conductors not transposed is converted in terms of the resistivity of the soil. The positive-sequence resistance for conductors transposed is given in (24), at the bottom of the page, and for conductors not transposed are shown as follows:

$$R_{1(NT\_\rho)} = A_{21} + \left[A_{22} / \left\{ A_{82} + A_{83}L_2 + A_{84}L_2^2 \right\} \right] \quad (25)$$

where $L_2 = \ln(\rho)$.

By varying the resistivity over a wide range, the positive-sequence resistance for both alternatives is plotted as in Fig. 7.

F. Operating the Three Cables at the Same Temperature

The operating temperature of the three cables is approximately the same. In this subsection, it is considered that the temperature of conductors and wires is the same. Therefore, the 6×6 primitive matrix simplifies to

$$Z_{\mathrm{primitive}} = \begin{bmatrix} Z_{\mathrm{c}} & Z_m & Z_m & Z_{\mathrm{cw}} & Z_{\mathrm{m}} & Z_{\mathrm{m}} \\ Z_{\mathrm{m}} & Z_{\mathrm{c}} & Z_{\mathrm{n}} & Z_{\mathrm{m}} & Z_{\mathrm{cw}} & Z_{\mathrm{n}} \\ Z_{\mathrm{m}} & Z_{\mathrm{n}} & Z_{\mathrm{c}} & Z_{\mathrm{m}} & Z_{\mathrm{n}} & Z_{\mathrm{cw}} \\ Z_{\mathrm{cw}} & Z_{\mathrm{m}} & Z_{\mathrm{m}} & Z_{\mathrm{w}} & Z_{\mathrm{m}} & Z_{\mathrm{m}} \\ Z_{\mathrm{m}} & Z_{\mathrm{cw}} & Z_n & Z_{\mathrm{m}} & Z_w & Z_n \\ Z_{\mathrm{m}} & Z_{\mathrm{n}} & Z_{\mathrm{cw}} & Z_{\mathrm{m}} & Z_{\mathrm{n}} & Z_{\mathrm{w}} \end{bmatrix} . \quad (26)$$

$$R_{1(T\_\rho)} = \frac{\left\{ A_{72} + L_2 \left[A_{73} + L_2 \left[A_{74} + L_2 \left[A_{75} + \left[A_{76} + A_{77}L_2 \right] L_2 \right] \right] \right] \right\}}{\left\{ A_{78} + L_2[A_{79} + A_{80}L_2] - A_{81} \ln \left(\rho^{\frac{3}{2}} \right) \right\}} \quad (24)$$

Conductor diameter = 7.34 mm
Conductor shield diameter = 8.636 mm
Insulation diameter = 21.84 mm
Insulation shield diameter = 23.37 mm
Concentric wires, copper 13 AWG 12
Jacket diameter = 30.23 mm
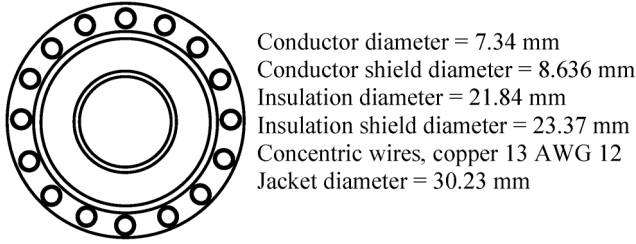
Fig. 8. Construction details of the 25-kV TRXLPE URD cable.

Conductor diameter = 8.26 mm
Conductor shield diameter = 9.65 mm
Insulation diameter = 30.00 mm
Insulation shield diameter = 33.27 mm
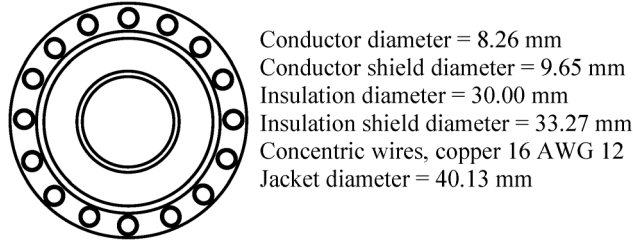Concentric wires, copper 16 AWG 12
Jacket diameter = 40.13 mm

Fig. 9. Construction details of the 35-kV TRXLPE URD cable.

Note that there are only four distinctive values for the elements of matrix (26) that are calculated as follows:

$$Z_c = (r + k_1 f) + jk_2 f \ln\left(\frac{k_3}{\alpha R}\sqrt{\frac{\rho}{f}}\right) :\Leftrightarrow r + R_m + jX_c$$

$$Z_w = (r_w + k_1 f) + jk_2 f \ln\left(\frac{k_3}{\mathrm{GMR}w}\sqrt{\frac{\rho}{f}}\right) :\Leftrightarrow r_w$$
$$+ R_m + jX_w$$

$$Z_{cw} = k_1 f + jk_2 f \ln\left(\frac{k_3}{\mathrm{GMR}w}\sqrt{\frac{\rho}{f}}\right) :\Leftrightarrow R_m + jX_w$$

$$Z_m = k_1 f + jk_2 f \ln\left(\frac{k_3}{d}\sqrt{\frac{\rho}{f}}\right) :\Leftrightarrow R_m + jA\ln\left(\frac{B}{d}\right)$$

$$Z_n = k_1 f + jk_2 f \ln\left(\frac{k_3}{2d}\sqrt{\frac{\rho}{f}}\right) :\Leftrightarrow R_m + jA\ln\left(\frac{B}{2d}\right). \quad (27)$$

Although the equations are simpler, it is not possible to obtain a sufficiently simple equation to see what parameter is responsible for the increase in the positive-sequence resistance.

IV. EXAMPLES OF CABLES

The parametric equations for cables with transposed conductors and with nontransposed conductors (14) are derived for a typical 220-kV installation used in [1]. To check the validity of these equations with distribution cables, a 25-kV and a 35-kV TRXLPE URD cable are considered.

The construction of the 25-kV TRXLPE URD cable is as shown in Fig. 8. and that of the 35-kV TRXLPE URD cable is as shown in Fig. 9. For both examples, the three cables are considered in a flat formation, separated by a distance of 0.1 m.
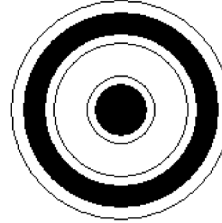

230 kV, conductor area = 506.7 mm^2
Conductor, copper, D=28.5 mm
Conductor shield, D = 31.4 mm
Insulation, XLPE (unfilled), D=77.9 mm
Insulation screen, D=80.2 mm
Corrugated sheath, copper, D=95.3 mm
Jacket, polyethylene, D=102.4 mm

Fig. 10. Cable 1: Construction details for a 230-kV XLPE, copper conductor, welded copper corrugated sheath cable.

230 kV, conductor area = 506.7 mm^2
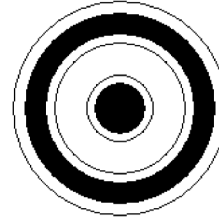Conductor, aluminum, D=28.5 mm
Conductor shield, D = 31.4 mm
Insulation, XLPE (unfilled), D=77.9 mm
Insulation screen, D=80.2 mm
Corrugated sheath, aluminum, D=98.2 mm
Jacket, polyethylene, D=105.3 mm

Fig. 11. Cable 2: Construction details of 230-kV XLPE, aluminum conductor, aluminum–corrugated sheath cable.

15 kV, conductor area = 33.62 mm^2
Conductor, copper, D=6.55 mm
Conductor shield, D = 7.7 mm
Insulation, XLPE (unfilled), D=16.6 mm
Insulation screen, D=18.1 mm
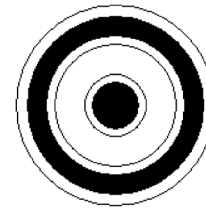Metallic sheath, copper tape, D=18.3 mm
Jacket, PVC, D=21.6 mm

Fig. 12. Cable 3: Construction details of 15 kV, copper conductor TRXLPE insulation, and longitudinal copper tape shielded cable.

With the 25-kV cable, the positive-sequence resistance for the transposed conductor is 0.5804 Ω/km whereas for the nontransposed conductor, it is 0.5786 Ω/km. For the 35-kV cable, the positive-sequence resistance calculated is 0.4664 Ω/km and 0.4644 Ω/km for cables with conductors transposed and conductors nontransposed, respectively. Thus, the positive-sequence resistance in both cables is higher for the transposed conductor than for the nontransposed conductors.

Three additional cables with different constructions are used to show the behavior of the positive-sequence resistance when the resistance of the shielding systems (sheath or concentric wires) in the cables varies. Cable 1 has a corrugated copper sheath (Fig. 10), cable 2 has a corrugated aluminum sheath (Fig. 11), and cable 3 has a moisture barrier design, including a longitudinally folded copper tape (Fig. 12). Each cable is laid in a flat formation arrangement as shown in Fig. 1. The positive-sequence resistance for conductors transposed and nontransposed for the three cables is given in Table I.

For cable 1 and cable 2, with different sheath resistances, the positive-sequence resistance when the conductors are transposed is found to be greater, by about 2.5%, than the positive-sequence resistance when the conductors are nontransposed. For

TABLE I
POSITIVE-SEQUENCE RESISTANCE FOR CABLES WITH CONDUCTORS
TRANSPOSED AND FOR CABLES WITH CONDUCTORS NONTRANSPOSED

Cable	R_1 Conductors Transposed (Ω/km)	R_1 Conductors Non-transposed (Ω/km)
1	0.0496	0.0483
2	0.0795	0.0777
3	0.6996	0.6994

TABLE II
VALUES OF α FOR CONDUCTORS [5]

Number of wires	α
1 (solid)	0.779
3	0.678
7	0.726
19	0.758
37	0.768
61	0.772
91	0.774
127	0.776

cable 3, as the copper tape sheath is very thin, the positive-sequence resistance changes very little when the conductors are transposed.

IEEE Standard 575 is currently under revision by the Insulated Conductors Committee (ICC); Draft 12 was made available to us. The conclusions of the sections related to our work remain similar to the current (1988) standard. In fact, Draft 12 has an expanded explanation of cross-bonded cables with conductor transposition. Our findings are not reflected. We will be working with the Working Group C2W Guide for High Voltage Cable Sheath Bonding (P575).

V. CONCLUSIONS

In this paper, we have found that conductor transposition for cross-bonded cables has technical disadvantages with respect to the case where the conductors are not transposed. Much larger losses can be produced when the conductors are transposed. Analytical formulas have been obtained for the calculation of the positive-sequence resistance. Through parametric analysis, it has been demonstrated that the positive-sequence resistance of cables with transposed conductors is always larger than that of cables with nontransposed conductors. We have varied the separation distance between cables, the insulation thickness, the number of concentric wires, the resistance of the conductors, and the resistivity of the soil. Examples of transmission and distribution cables have been discussed, including different constructions for sheath and screens. In all cases, except for sheaths with longitudinal copper tapes where losses remain the same, conductor transposition produces larger losses.

APPENDIX

$L = \ln\left(\frac{1}{d}\right)$	$A_1 = 3f\,k_1 + r_w$
$A_2 = f^2 k_2^2$	$A_3 = \ln(2)$
$A_4 = 8.99509 \times 10^8$	$A_5 = -8.12557 \times 10^8$
$A_6 = 2.55107 \times 10^8$	$A_7 = -1.92355 \times 10^7$
$A_8 = -4.52198 \times 10^6$	$A_9 = 5.21213 \times 10^5$
$A_{10} = 5.10368 \times 10^4$	$A_{11} = 60.2635$
$A_{12} = -34.0596$	$A_{13} = 5.47455$
$A_{14} = 4640.29$	$A_{15} = -2622.59$
$A_{16} = 421.54$	$A_{17} = 184151$
$A_{18} = -323.811$	$A_{19} = 3.23988 \times 10^4$
$A_{20} = 1401.49$	$A_{21} = 0.01578$
$A_{22} = 7.22844 \times 10^{-4}$	$A_{23} = 26.8912$
$A_{24} = 4.63657$	$A_{25} = 0.204656$
$A_{26} = 8.77904 \times 10^9$	$A_{27} = 3.63245 \times 10^9$
$A_{28} = 3.82796 \times 10^8$	$A_{29} = 1.65231 \times 10^7$
$A_{30} = 3.95267 \times 10^6$	$A_{31} = 12759.196$
$A_{32} = 460293.3881$	$A_{33} = 26110.8022$
$A_{34} = 6408.77042$	$A_{35} = 421.54046$
$A_{36} = 2.49734$	$A_{37} = 339.10128$
$A_{38} = 83.23078$	$A_{39} = 5.474551$
$A_{40} = 0.032433$	$A_{41} = 285758.53205$
$A_{42} = 19860.427924$	$A_{43} = 350.371293$
$A_{44} = 0.64127$	$A_{45} = 0.017054$
$A_{46} = 42.83705$	$A_{47} = 15.20321$
$A_{48} = 9.1309 \times 10^9$	$A_{49} = 1.79514 \times 10^7$
$A_{50} = 3.63246 \times 10^9$	$A_{51} = 3.82797 \times 10^8$
$A_{52} = 1.65232 \times 10^7$	$A_{53} = 3.95268 \times 10^6$
$A_{54} = 12759.2$	$A_{55} = 166081$
$A_{56} = 15056.9$	$A_{57} = 350.371$
$A_{58} = 24942.2$	$A_{59} = 6408.77$
$A_{60} = 421.54$	$A_{61} = 194.793$
$A_{62} = 323.925$	$A_{63} = 83.2308$
$A_{64} = 5.47455$	$A_{65} = 2.52978$
$A_{66} = 24.2525$	$A_{67} = 2.19873$
$A_{68} = 0.051164$	$A_{69} = 0.00289512$
$A_{70} = 0.999999$	$A_{71} = 2.33112 \times 10^{-5}$
$A_{72} = 1.97168 \times 10^8$	$A_{73} = 3.25635 \times 10^7$
$A_{74} = 1.39886 \times 10^6$	$A_{75} = 0.124769$
$A_{76} = 3.77841 \times 10^{-3}$	$A_{77} = 4.31619 \times 10^{-5}$
$A_{78} = 1.05578 \times 10^{10}$	$A_{79} = 1.78984 \times 10^9$
$A_{80} = 7.49049 \times 10^7$	$A_{81} = 3.07675 \times 10^7$
$A_{82} = 16.226$	$A_{83} = 2.67982$
$A_{84} = 0.115119$	

REFERENCES

[1] F. de León, M. Márquez-Asensio, and G. Álvarez-Cordero, "Effects of conductor counter-transposition on the positive sequence impedance and losses of cross-bonded cables," *IEEE Trans. Power Del.*, vol. 26, no. 3, pp. 2060–2063, Jul. 2011.

[2] *IEEE Guide for the Application of Sheath-Bonding Methods for Single-Conductor Cables and the Calculation of Induced Voltages and Currents in Cable Sheaths*, ANSI/IEEE Standard 575-1988, 1988.

[3] W. H. Kersting, *Distribution System Modeling and Analysis*. Boca Raton, FL: CRC, 2002.

[4] *Electric cables—Calculation of the current rating—Part 1–1: Current rating equations (100% load factor) and calculation of losses. General*, IEC Standard 60287-1-1, 2001, Ed. 1.2, 2001-11.

[5] *Electric cables—Calculation of the current rating—Part 1–3: Current rating equations (100% load factor) and calculation of losses. Current sharing between parallel single-core cables and calculation of circulating current losses*, IEC Standard 60287-1-3, 2002, 1st Ed. 2002-05.

Prajakta Moghe received the B.E. degree in electronics engineering from Mumbai University (K. J. Somaiya College of Engineering), Maharashtra, India, in 2010 and the M.S. degree in electrical engineering from Polytechnic Institute of New York University, Brooklyn, NY, USA, in 2012.

Her research interests include power system economics and study of cables.

Francisco de León (S'86–M'92–SM'02) received the B.Sc. and the M.Sc. (Hons.) degrees in electrical engineering from the National Polytechnic Institute, Mexico City, Mexico, in 1983, and 1986, respectively, and the Ph.D. degree in electrical engineering from the University of Toronto, Toronto, ON, Canada, in 1992.

He has held several academic positions in Mexico and has worked for the Canadian electric industry. Currently, he is an Associate Professor at the Polytechnic Institute of NYU, Brooklyn, NY. His research interests include the analysis of power definitions under nonsinusoidal conditions, the transient and steady-state analyses of power systems, the thermal rating of cables and transformers, and the calculation of electromagnetic and thermal fields applied to machine design and modeling.